

Probing spontaneous wave-function collapse with entangled levitating nanospheresJing Zhang,^{1,2} Tiancai Zhang,^{1,2} and Jie Li^{1,2,3}¹*State Key Laboratory of Quantum Optics and Quantum Optics Devices, Institute of Opto-Electronics, Shanxi University, Taiyuan 030006, China*²*Collaborative Innovation Center of Extreme Optics, Shanxi University, Taiyuan 030006, China*³*School of Science and Technology, Physics Division, University of Camerino, I-62032 Camerino (MC), Italy*

(Received 4 December 2016; published 30 January 2017)

Wave-function collapse models are considered to be the modified theories of standard quantum mechanics at the macroscopic level. By introducing nonlinear stochastic terms in the Schrödinger equation, these models (different from standard quantum mechanics) predict that it is fundamentally impossible to prepare macroscopic systems in macroscopic superpositions. The validity of these models can only be examined by experiments, and hence efficient protocols for these kinds of experiments are greatly needed. Here we provide a protocol that is able to probe the postulated collapse effect by means of the entanglement of the center-of-mass motion of two nanospheres optically trapped in a Fabry-Pérot cavity. We show that the collapse noise results in a large reduction of the steady-state entanglement, and the entanglement, with and without the collapse effect, shows distinguishable scalings with certain system parameters, which can be used to determine unambiguously the effect of these models.

DOI: [10.1103/PhysRevA.95.012141](https://doi.org/10.1103/PhysRevA.95.012141)**I. INTRODUCTION**

Wave-function collapse models (CMs) [1], as the modified theories of standard quantum mechanics, postulate a fundamental breakdown of quantum superposition at the macroscopic scale. They have been proposed to explain the lack of observations of macroscopically distinguishable superposition states of macroscopic objects, and they offer a possible solution to the quantum measurement problem [2] and the quantum-to-classical transition. There are several different versions of CMs, e.g., the Ghirardi-Rimini-Weber approach [3], continuous spontaneous localization (CSL) [4], and gravitationally induced CMs [5]. These models modify the Schrödinger equation by introducing appropriate stochastic nonlinear terms, of which the effect is negligible for microscopic systems while it becomes prominent for macroscopic objects, resulting in the emergence of macroscopic classicality.

Many proposals have been put forward to examine these CMs in different systems and with different approaches. In general, they can be divided into two kinds: an interferometric approach and a noninterferometric approach. For the former, matter-wave interferometry [6] is typically used, where large massive objects, e.g., molecules or clusters [7], are sent through interference gratings. However, to date the mass range has not been reached to effectively test the CMs. For the latter, protocols [8–13] have been recently provided based on cavity optomechanics [14]. The main advantage of this approach is that the preparation of large spatial superposition states [15–18] is not required. It has been shown [8–10,12] that collapse noise induced momentum diffusion of a mechanical resonator (MR) could be probed in the phase noise of the cavity output light. Apart from the above, more recently quantum estimation theory has been applied to discriminate the effect of CMs [19,20].

In this paper, we provide a scheme to test the CMs by means of the steady-state entanglement of two macroscopic MRs. Many protocols have been proposed for the generation of entanglement between two massive MRs using optome-

chanical and/or electromechanical systems, e.g., by exploiting radiation pressure [21–24], by transferring entanglement [25–27] or squeezing [28] from optical fields, by conditional measurements on light modes [29–34], and by reservoir engineering realized by properly choosing multifrequency drivings [35–41]. We will focus on the CSL model, which is one of the most widely studied CMs. The scheme is based on the known fact that entanglement, as a kind of quantum correlation, is particularly sensitive to various noises. A small increase in noise may significantly degrade the entanglement. As is known, the collapse noise postulated in the CMs is typically very small, thus bringing about challenges for experimental verification. In view of these facts, entanglement could act as a perfect probe that may be able to sense whether the collapse noise is present or not. The reason we adopt *steady-state* entanglement is that, in order to efficiently test the CMs, one should prepare entangled states that last for a relatively long time [42,43]. We know that entanglement in steady states, rather than in transient states, is harder to prepare due to the continuous decoherence process interacting with various noises. The effect of the CMs would be more noticeable in the steady-state entanglement due to the time accumulation effect.

The system used to test the collapse theories should possess environmental noises that are as small as possible, comparable to the hypothetical collapse noise, and the test object should be large or massive enough to yield a considerable collapse effect. Levitated nanospheres [16,44–48], possessing very high mechanical quality factors, could be the ideal platform to implement such a test. Protocols [12,13] have been provided using a single nanosphere trapped in a Fabry-Pérot optical cavity that are able to test the strength of the collapse rate in the CSL theory to values as low as 10^{-12} Hz with realistic parameters. In the present paper, we study the effect of the CSL on quantum correlations of two macroscopic objects. Specifically, we employ two nanospheres optically trapped in a Fabry-Pérot cavity, and we study the CSL effect on the stationary entanglement of the center-of-mass motion of the

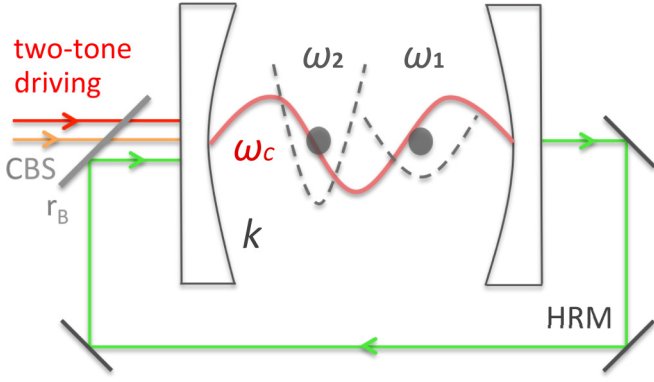


FIG. 1. Sketch of the proposed scheme for testing the CSL theory with entangled nanospheres. Two identical nanospheres are optically trapped with different frequencies ω_1 and ω_2 in a Fabry-Pérot cavity. The cavity mode is bichromatically driven at the two frequencies $\omega_0 + \omega_1$ and $\omega_0 - \omega_2$. Large and robust entanglement between the two spheres can be generated in the steady state. The output field of the cavity is fed back into the input port through highly reflective mirrors (HRMs) and a controllable beamsplitter (CBS) with a tunable reflection coefficient r_B , which is used for reducing the cavity loss and improving the entanglement.

two spheres. Since the entanglement is particularly sensitive to noises, the diffusion rates of various noises in the system must be small. We find that, with properly chosen parameters, the collapse noise results in a large reduction of the entanglement, and the entanglement shows distinguishable scalings, with and without the CSL effect, with certain system parameters, e.g., the trapping frequency, due to the fact that different sources of noise exhibit different scalings with the system parameters [12]. The above observation can determine unambiguously whether the collapse noise is actually present or effective.

The remainder of the paper is organized as follows: In Sec. II, we describe our system in detail, we provide the quantum Langevin equations for achieving the entanglement of the two nanospheres, and we analyze the diffusion rates of various noises (both environmental and the postulated collapse noise) in the system. In Sec. III, we present the results and show the details of the parameters with which the CSL effect and the corresponding value of the collapse rate could be determined. Finally, Sec. IV is devoted to conclusions and discussions, and the Appendix gives the details for calculating the steady-state entanglement.

II. THE SYSTEM

Before constructing the test, we shall first prepare two nanospheres into entangled states. We adopt the scheme provided in Ref. [41], which is able to generate large and robust entanglement between two MRs in steady states. As depicted in Fig. 1, we consider two identical spheres of radius R trapped by harmonic dipole traps with different frequencies ω_1 and ω_2 in two different potential wells within a Fabry-Pérot cavity. The center-of-mass motion of the sphere is modeled as a quantum-mechanical harmonic oscillator. The cavity is of length L , finesse \mathcal{F} , and mirror radius of curvature R_c . A single cavity mode with resonance frequency ω_c , interacting

via the usual optomechanical interaction with the two MRs, is bichromatically driven, with powers P_1 and P_2 , at the two sideband frequencies $\omega_{L1} = \omega_0 + \omega_1$ and $\omega_{L2} = \omega_0 - \omega_2$ with the reference frequency ω_0 detuned from the cavity resonance by $\Delta_0 = \omega_c - \omega_0$. This means that the cavity mode is simultaneously driven close to the blue sideband associated with the first MR and close to the red sideband associated with the second MR. We note that the scheme [41] is an improved version of the one [40] in which a coherent feedback loop is introduced, which leads to a significantly reduced effective cavity decay rate and a remarkable improvement in the entanglement. This is vital and makes it possible to test the CMs based on this scheme because the mechanical frequency $\omega_{1,2}$ can now take much smaller values (since the effective cavity decay rate κ_{eff} is significantly reduced due to the feedback) to fulfill the condition of the scheme, $\kappa_{\text{eff}} \ll \omega_{1,2}, |\omega_1 - \omega_2|$ [40]. As shown in Ref. [12], the diffusion rate D_t due to the scattering of trapping light, which will be the main diffusion for the system at low pressure and temperature, is proportional to the trapping frequency $\omega_{1,2}$. A much smaller $\omega_{1,2}$ yields a much smaller diffusion rate D_t , making it possible to generate sizable stationary entanglement between the two MRs.

The system dynamics can be efficiently studied by linearizing the optomechanical interaction in the limit of a large driving field. The relevant degrees of freedom for the linearized dynamics are the fluctuations of the cavity field and of the mechanical center-of-mass variables about their respective average values, described by the amplitude and phase quadratures X and Y (with $[X, Y] = i$) of the cavity field, and by the dimensionless position and momentum x_j and p_j (with $[x_j, p_j] = i, j=1,2$) of the nanospheres. The corresponding quantum Langevin equations, in the interaction picture with respect to $H_0 = \hbar\omega_0(X^2 + P^2)/2 + \hbar \sum_{j=1,2} \omega_j(x_j^2 + p_j^2)/2$, are given by [40,41]

$$\begin{aligned} \dot{X} &= -\kappa_{\text{eff}} X - G_1 p_1 + G_2 p_2 + \sqrt{2\kappa_{\text{eff}}} X^{\text{in}}, \\ \dot{Y} &= -\kappa_{\text{eff}} Y - G_1 x_1 - G_2 x_2 + \sqrt{2\kappa_{\text{eff}}} Y^{\text{in}}, \\ \dot{x}_j &= -\frac{\gamma}{2} x_j + (-1)^j G_j Y + F_x^j, \\ \dot{p}_j &= -\frac{\gamma}{2} p_j - G_j X + F_p^j, \end{aligned} \quad (1)$$

where we have set the effective detuning $\Delta = \Delta_0 + \delta$ (δ is the frequency shift due to the optomechanical interaction and also the feedback) equal to zero, which is the optimal detuning for the generation of entanglement [41]. $\kappa_{\text{eff}} = \kappa(1 - |r_B| \cos \theta)$ is the effective cavity decay rate due to the coherent feedback, where r_B is the reflection coefficient of the controllable beamsplitter in the feedback loop (see Fig. 1), θ is the phase shift of the light in the feedback loop, and $\kappa = \pi c / (2\mathcal{F}L)$ (c the speed of light) is the cavity decay rate without feedback. We see that κ_{eff} can be significantly reduced when $|r_B| \rightarrow 1$ and $\theta = 2n\pi$ ($n = 0, 1, 2, \dots$). In practice, one can always adjust this phase shift and set it equal to the optimal value for the entanglement $\theta = 2n\pi$ [41]. $G_j = g_j \alpha_j$ is the effective optomechanical coupling, where $\alpha_j = \sqrt{2\kappa_{\text{eff}} P_j / [\hbar\omega_{Lj}(\omega_j^2 + \kappa_{\text{eff}}^2)]}$, and $g_j = \omega_c \sqrt{\frac{\hbar}{m\omega_j} \frac{2\pi}{\lambda_c} \frac{\epsilon-1}{\epsilon+2} \frac{3V_s}{4V_c}}$ [44] is the bare optomechanical coupling associated with the j th MR, where λ_c is the cavity wavelength,

ϵ is the electric permittivity of the sphere, V_s is its volume, and $V_c = \pi L W_0^2 / 4$ is the cavity mode volume with mode waist $W_0 = \sqrt{\lambda_c L (2R_c/L - 1)^{1/2} / 2\pi}$. $\gamma = \frac{16}{\pi} \frac{P_a}{\bar{v} R \rho_0}$ is the mechanical damping rate due to the friction with residual air molecules, with P_a the gas pressure, ρ_0 the mass density of the sphere, $\bar{v} = \sqrt{3k_B T / m_a}$ the mean speed of the air molecules, m_a their mass (which we take to be $m_a = 28.97$ amu), and T the gas temperature [44]. For levitated nanospheres, γ can be very small, leading to very high quality factors, $\gtrsim 10^{10}$ [49]. X^{in} and Y^{in} are the quadratures of the vacuum noise entering into the cavity, and their only nonzero correlation functions are

$$\langle X^{\text{in}}(t) X^{\text{in}}(t') \rangle = \langle Y^{\text{in}}(t) Y^{\text{in}}(t') \rangle = \frac{1}{2} \delta(t - t'). \quad (2)$$

F_x^j and F_p^j are the combined force operators in the rotating frame, which include all the relevant stochastic forces accounting for the mechanical diffusion. The only nonzero correlation functions are

$$\begin{aligned} \langle F_x^j(t) F_x^j(t') \rangle &= \langle F_p^j(t) F_p^j(t') \rangle \\ &= \frac{1}{2} \delta_{j,j'} \delta(t-t') (D_a^j + D_t^j + D_c^j + \lambda_{\text{sph}}^j), \end{aligned} \quad (3)$$

where D_a^j , D_t^j , D_c^j , and λ_{sph}^j are, respectively, the diffusion rates caused by the scattering of background air molecules, of trapping light, of cavity photons, and by the collapse noise. In the relevant high-temperature limit, D_a^j is given by

$$D_a^j = 2\gamma \frac{k_B T}{\hbar \omega_j}. \quad (4)$$

The diffusion rates due to the scattering of trapping and cavity light are given, respectively, by [50]

$$D_t^j = \frac{8\epsilon_c^2 k_c^6 R^3}{9\rho_0 \omega_j} \frac{\mathcal{I}_j}{\omega_{Lt}}, \quad D_c^j = \frac{2\epsilon_c^2 k_c^6 R^3}{9\rho_0 \omega_j} \frac{\hbar n_{\text{ph}c}}{V_c}, \quad (5)$$

where $\epsilon_c = 3 \frac{\epsilon-1}{\epsilon+2}$, $k_c = 2\pi/\lambda_c$, ω_{Lt} is the frequency of the trapping laser, and \mathcal{I}_j is the intensity of the trapping field, which is given by $\mathcal{I}_j = P_{tj}/(\pi W_t^2)$. P_{tj} is the laser power and W_t is the waist of trapping light, which is approximated by $W_t \approx \lambda_c/(\pi \mathcal{N})$, with \mathcal{N} the numerical aperture, and the trapping frequency is determined by $\omega_j = [4\epsilon_c \mathcal{I}_j / (\rho_0 c W_t^2)]^{1/2}$. Finally, $n_{\text{ph}} = |\alpha_1|^2 + |\alpha_2|^2$ is the mean cavity photon number.

According to the CSL theory, the collapse noise induced diffusion rate for a spherical particle is given by [9]

$$\lambda_{\text{sph}}^j = \frac{\hbar}{\omega_j} \frac{8\pi \lambda \rho_0}{m_0^2} \left[e^{-R^2/r_c^2} - 1 + \frac{R^2}{2r_c^2} (e^{-R^2/r_c^2} + 1) \right] \frac{r_c^4}{R^3}, \quad (6)$$

with m_0 the atomic mass unit. The actual strength of the collapse noise is determined by two phenomenological parameters: the characteristic length r_c and the collapse rate λ . The characteristic length is typically set at $r_c \simeq 100$ nm, above which the collapse effect tends to be prominent. λ denotes the average collapse rate at one proton mass. The initial estimate of λ is 10^{-16} Hz [3,4], while larger values have been proposed, e.g., $10^{-8 \pm 2}$ Hz given by Adler [51]. Up to now, different experiments have indicated that λ should be lower than $\sim 10^{-8}$ Hz [52–56], $\sim 10^{-9}$ Hz [57], and $\sim 10^{-11}$ Hz

TABLE I. Different scalings of the diffusion rates D_t , D_c , D_a , and λ_{sph} with two key parameters of the system, i.e., the radius of the sphere R and the trapping frequency ω . The symbol “ \uparrow ” (“ $=$ ”) denotes an increasing (constant) function of the parameter.

Parameter	D_t	D_c	D_a	λ_{sph}
R	$\propto R^3$	= (fixed G)	$\propto R^{-1}$	\uparrow ($R < 2.38r_c$)
ω	$\propto \omega$	= (fixed G)	$\propto \omega^{-1}$	$\propto \omega^{-1}$

[58] for $r_c \simeq 100$ nm. Does an exact value or range of λ exist, and if so, how large is it? These questions can only be answered by experiments.

III. TEST OF THE CSL THEORY WITH ENTANGLED NANOSPHERES

We observe that D_t , $D_c \propto R^3$ (D_c is, however, independent of R for fixed values of G), λ_{sph} increases with R when $R < 2.38r_c$, while $D_a \propto 1/R$, as displayed in Table I. Since the entanglement is particularly sensitive to various noises, implying that a relatively small size of the sphere should be adopted, we consider the radius of the sphere $R = 0.15 - 0.22r_c$ (while a larger size $R = r_c$ has been used in Ref. [12], where the observable is instead the phase quadrature of the output light), which yields not large D_t , D_c , and D_a , and comparable λ_{sph} , as shown in Fig. 2(a). We have taken a value of G_2 that is as small as possible (the ratio of G_1/G_2 is, however, optimized for the entanglement [40,41]), which gives a negligible D_c but is large enough to generate sizable entanglement. Another reason $G_{1,2}$ must be small is that in order to make the scheme of Ref. [41] valid, $G_{1,2} \ll \omega_{1,2}, |\omega_1 - \omega_2|$ must be fulfilled [40]. We have also assumed the system is at low temperature, $T = 10$ mK, and pressure, $P_a = 10^{-12}$ Torr, resulting in a sufficiently small D_a . Figure 2 is plotted as a function of the mechanical frequency $\omega_{1,2}$, which is a key parameter [12] and can be easily altered by adjusting the intensity of the trapping laser. Under these conditions, one could see two distinguishable curves of the total diffusion rate with and without the CSL effect [see Fig. 2(b)], which thereby result in distinguishable curves of the entanglement (see the Appendix for calculating the steady-state entanglement), as shown in Fig. 2(c). We see that the entanglement in the absence of the CSL effect decreases almost linearly with $\omega_{1,2}$, while it increases first and then decreases with the CSL effect, and more noticeably, the difference of their values in these two cases is quite large, confirming the sensitivity of the entanglement to the noise. Therefore, the CSL effect could be determined by repeating the experiment at different trapping laser powers and verifying the distinguishable behavior, particularly the different signs of the slope of the curves, in the region of small $\omega_{1,2}$.

In Fig. 3 we present the results for testing the CSL with different collapse rates $\lambda = 10^{-9}$, 10^{-10} , and 10^{-11} Hz. As λ decreases, the CSL effect becomes weaker and weaker. To amplify this effect, we employ bigger and bigger spheres, R from $0.15r_c$ to $0.22r_c$, so that λ_{sph} is enlarged while D_t is not increased too much, retaining nonzero entanglement. In this process, D_a is no longer negligible and starts to

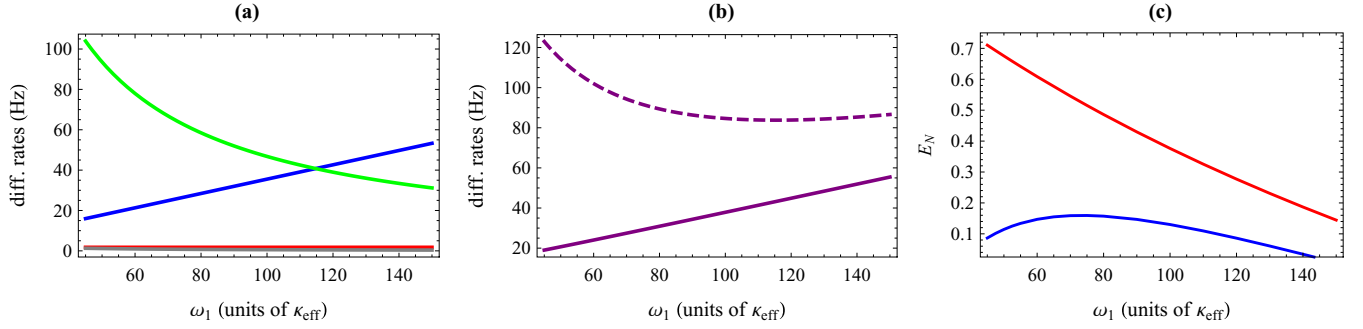


FIG. 2. (a) Diffusion rates for the scattering of trapping light D_t^1 (blue), cavity light D_c^1 (red), air molecules D_a^1 (gray), and the collapse rate λ_{sph}^1 (green) vs the trapping frequency ω_1 . Note that the curves of D_c^1 and D_a^1 are very close to the ω_1 axis and are no longer visible. (b) The solid line denotes the sum of the diffusion rates D_t^1 , D_c^1 , and D_a^1 in (a), while the dashed line includes also the collapse rate λ_{sph}^1 on the basis of the solid line. (c) Steady-state entanglement E_N between the two nanospheres vs the trapping frequency ω_1 . The blue (red) line refers to the case with (without) the CSL effect. The parameters are $R = 0.15r_c$, $r_B = 0.99$, $G_2 = 1.2\kappa_{\text{eff}}$, $G_1 = 0.72G_2$, $\omega_2 = 2\omega_1$, $L = 4$ cm, $\kappa = 20$ kHz (corresponding to $\mathcal{F} = 5.9 \times 10^5$ and $\kappa_{\text{eff}} = 200$ Hz), $R_c = L/1.5$, $\lambda_c = 1064$ nm, $\mathcal{N} = 0.8$, $T = 10$ mK, $P_a = 10^{-12}$ Torr, $\lambda = 10^{-8}$ Hz, $r_c = 100$ nm, and we use diamond nanospheres with $\rho_0 = 3.5$ g/cm³ and $\epsilon = 5.76$.

play its role, making the solid lines in Figs. 3(a)–3(c) less and less linear, especially when $\omega_{1,2}$ is small. Since it has the same scaling as λ_{sph} versus $\omega_{1,2}$, i.e., D_a , $\lambda_{\text{sph}} \propto 1/\omega_{1,2}$ (see Table I), its value, depending on the gas temperature and pressure, will be the most relevant factor that eventually determines the value of the upper bound of λ that can be tested based on the system of levitated nanospheres, either optically or magnetically [59] trapped. Another efficient way to increase λ_{sph} and simultaneously decrease D_t is by lowering the trapping frequency $\omega_{1,2}$. However, the condition $\kappa_{\text{eff}} \ll \omega_{1,2}, |\omega_1 - \omega_2|$ limits the smallest value that $\omega_{1,2}$ can take, which, however, can be relaxed by reducing κ_{eff} implemented

by taking larger values of r_B . Even so, one should not consider taking too small values of $\omega_{1,2}$ because when the mechanical frequencies are too low, other unwanted electronic noises will enter into the system, making our scheme less effective. We see in Figs. 3(d)–3(f) that, as λ decreases, the distinguishability of the two curves with and without the CSL reduces. At $\lambda \sim 10^{-11}$ Hz, the two curves are no longer that distinguishable, nevertheless the difference of their values is still considerable (thanks to the powerful scheme in [40,41]). If the difference caused by all uncontrolled noises and system errors, e.g., due to the imprecision of measurements and of the calibration of the experimental parameters, is smaller than that

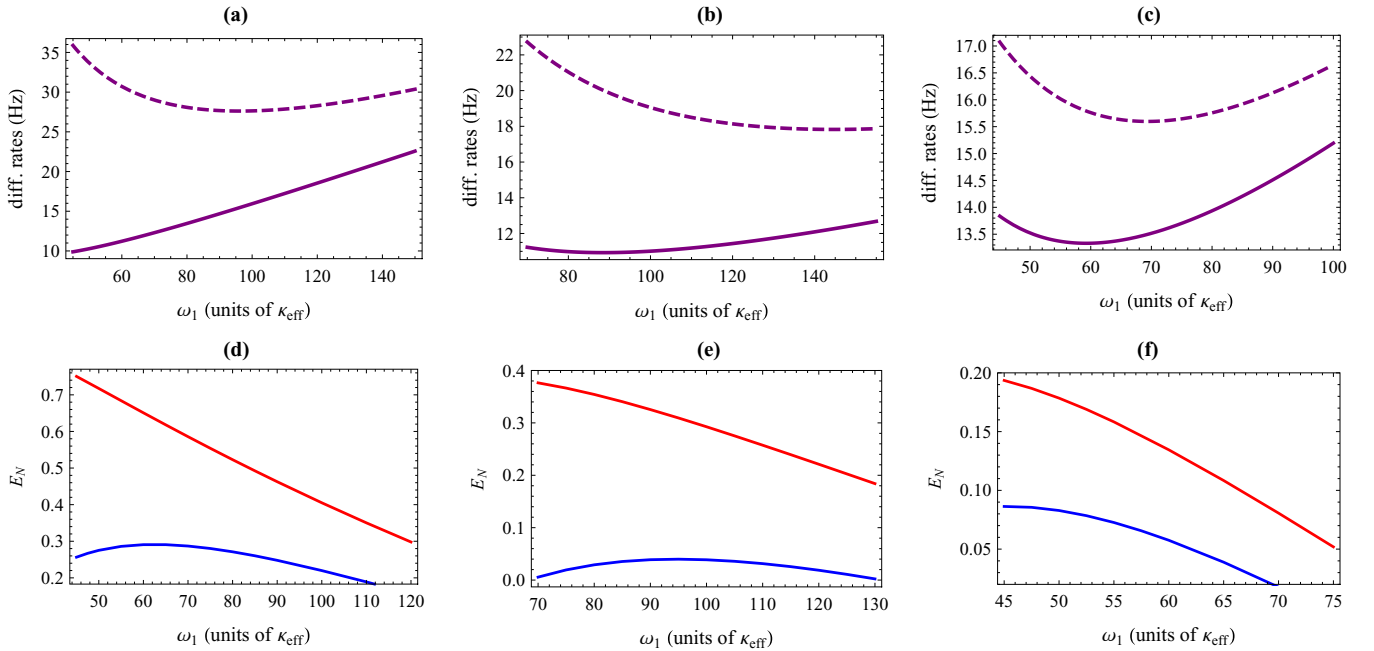


FIG. 3. (a)–(c) Total diffusion rates with (dashed line, i.e., $D_t^1 + D_c^1 + D_a^1 + \lambda_{\text{sph}}^1$) and without (solid line, i.e., $D_t^1 + D_c^1 + D_a^1$) the CSL effect vs the trapping frequency ω_1 . (d)–(f) Steady-state entanglement E_N of the two nanospheres vs the trapping frequency ω_1 . The blue (red) line corresponds to the case with (without) the CSL effect. The parameters are as follows: (a),(d) $\lambda = 10^{-9}$ Hz, $R = 0.15r_c$, $r_B = 0.996$, $G_2 = 1.2\kappa_{\text{eff}}$, $G_1 = 0.77G_2$. (b),(e) $\lambda = 10^{-10}$ Hz, $R = 0.18r_c$, $r_B = 0.999$, $G_2 = 2.2\kappa_{\text{eff}}$, $G_1 = 0.79G_2$. (c),(f) $\lambda = 10^{-11}$ Hz, $R = 0.22r_c$, $r_B = 0.999$, $G_2 = 2\kappa_{\text{eff}}$, $G_1 = 0.79G_2$. The other parameters are as in Fig. 2.

induced by the CSL effect [the relative difference between the two curves in Fig. 3(c), when ω_1 is small, is about 19%], one can determine the CSL effect with the collapse rate down to $\lambda \sim 10^{-11}$ Hz, and even lower.

We finally discuss how to detect the generated entanglement of the two nanospheres. We follow the detection scheme provided in Ref. [40], i.e., sending into the cavity two weak red-detuned probe fields with detunings, respectively, equal to the two mechanical frequencies, i.e., $\Delta_j^p = \omega_{cj} - \omega_j^p = \omega_j$ ($j = 1, 2$ and ω_{cj} are two other cavity resonance frequencies). The probe modes adiabatically follow the dynamics of the two MRs, and the output of the readout cavity a_j^{out} is given by [60]

$$a_j^{\text{out}} = i \frac{G_j^p}{\sqrt{\kappa_{\text{eff}}}} b_j + a_j^{\text{in}}, \quad j = 1, 2, \quad (7)$$

where $b_j = (x_j + ip_j)/\sqrt{2}$, G_j^p is the very small optomechanical coupling with the probe mode, and a_j^{in} denotes the input vacuum noise. Therefore, by homodyning the probe mode outputs from the transmission of the controllable beamsplitter (see Fig. 1), and by changing the phases of the corresponding local oscillator, the quadratures of the two MRs, $\{x_1, p_1, x_2, p_2\}$, are measured, and thus the covariance matrix of the quadratures is constructed, from which the entanglement can then be numerically obtained in the way introduced in the Appendix. The probe fields will also induce mechanical diffusion due to the scattering of photons, however it can be neglected if the probe fields are sufficiently weak. We have checked that in all the plots of Fig. 3, D_c is always negligible compared to other diffusion rates, which means that even if the power of the probe field is equivalent to that of the driving laser, the diffusion induced by it is also negligible.

IV. CONCLUSIONS AND DISCUSSIONS

We have suggested a scheme based on entangled levitating nanospheres to probe the possible effect of the CSL theory. Our scheme is designed for nanospheres optically trapped in Fabry-Pérot cavities, however it can also be applied to a system of magnetically trapped spheres, where diffusion due to the scattering of a trapping field will be significantly reduced [59]. We have shown that the steady-state entanglement of the center-of-mass motion of the two nanospheres is particularly sensitive to the noises in the system, and the CSL effect results in a remarkably large reduction of entanglement. The entanglement shows distinguishable scalings, with and without the CSL effect, with the system parameter of the trapping frequency for the collapse rate down to $\lambda \sim 10^{-10}$ Hz, while it starts to show similar scalings for $\lambda \sim 10^{-11}$ Hz, implying that our scheme can *unambiguously* determine the CSL effect for λ down to $\sim 10^{-10}$ Hz with realistic parameters, and it can also test it for $\lambda \sim 10^{-11}$ Hz, and even lower, if the difference of the entanglement caused by uncontrolled noises and the imprecision of measurements and parameter calibration is smaller than that induced by the CSL effect.

We notice that under the same conditions of temperature and pressure, $T = 10$ mK and $P_a = 10^{-12}$ Torr, the present scheme is not as efficient as the one provided in Ref. [12], where the observable is instead the phase of the cavity output light. This is because, as mentioned at the beginning in

Sec. III, in order to have sizable entanglement a relatively small size of the sphere is adopted, yielding a larger D_a (since $D_a \propto 1/R$). It eventually determines that this scheme, based on entanglement, could not *unambiguously* probe the CSL effect for λ down to 10^{-12} Hz, which, however, can be done using the scheme of Ref. [12]. One promising solution is to employ the system of magnetically trapped spheres, e.g., the proposal provided in Ref. [59], where a superconducting microsphere is magnetically trapped close to a quantum circuit. In contrast with optical levitation, the main diffusion due to the scattering of trapping light is absent, and the decoherence in the magnetic levitation system is predicted to be very small. The new system brings in additional sources of noise, e.g., due to hysteresis losses in the superconducting coils and fluctuations in the trap frequency and the trap center. However, all of them are predicted to be negligible [59]. Adopting such a magnetic levitation scheme, the entanglement could be generated with a (much) larger size of the spheres, which will significantly increase λ_{sph} while simultaneously reducing D_a . The CSL effect with λ well below 10^{-12} Hz, if is present, is expected to be probed with realistic parameters.

ACKNOWLEDGMENTS

This work has been supported by the National Natural Science Foundation of China (Grants No. 11504218, No. 11634008, No. 11674203, No. 91336107, and No. 61227902), and by the Major State Basic Research Development Program of China.

APPENDIX

Here we provide the details on how we obtain the steady-state entanglement between the two MRs. The entanglement is calculated based on the covariance matrix of the two mechanical modes. The covariance matrix can be achieved by solving the quantum Langevin equations (1), which can be rewritten in the following form:

$$\dot{U}(t) = \mathcal{A}U(t) + \mathcal{N}(t), \quad (\text{A1})$$

where $U(t)$ is the vector of quadrature fluctuation operators of the two mechanical modes and one cavity mode, i.e., $U(t) = (x_1(t), p_1(t), x_2(t), p_2(t), X(t), Y(t))^T$. \mathcal{A} is the drift matrix, which takes the form of

$$\mathcal{A} = \begin{pmatrix} -\frac{\gamma}{2} & 0 & 0 & 0 & 0 & -G_1 \\ 0 & -\frac{\gamma}{2} & 0 & 0 & -G_1 & 0 \\ 0 & 0 & -\frac{\gamma}{2} & 0 & 0 & G_2 \\ 0 & 0 & 0 & -\frac{\gamma}{2} & -G_2 & 0 \\ 0 & -G_1 & 0 & G_2 & -\kappa_{\text{eff}} & \Delta \\ -G_1 & 0 & -G_2 & 0 & -\Delta & -\kappa_{\text{eff}} \end{pmatrix}, \quad (\text{A2})$$

where Δ is the effective detuning (its exact expression is provided in Ref. [41]), and we take $\Delta = 0$ corresponding to the optimal detuning for the entanglement. The system is stable when all the eigenvalues of the drift matrix \mathcal{A} have negative real parts, which can be simply achieved when $|G_1| < |G_2|$ is fulfilled [41]. $\mathcal{N}(t)$ is the vector of noise quadrature operators associated with the noise terms in Eqs. (1).

The *steady-state* covariance matrix $V(t \rightarrow \infty)$ of the system quadratures, with its entries defined as $V_{ij} = \frac{1}{2} \langle \{U_i, U_j\} \rangle$ ($\{, \}$

denotes an anticommutator, and $i, j = 1, 2, \dots, 6$, is obtained by solving the Lyapunov equation

$$AV + VA^T = -\mathcal{D}, \quad (\text{A3})$$

where \mathcal{D} is the diffusion matrix, with its entries defined as

$$\frac{1}{2} \langle \mathcal{N}_i(t) \mathcal{N}_j(s) + \mathcal{N}_j(s) \mathcal{N}_i(t) \rangle = \mathcal{D}_{ij} \delta(t - s). \quad (\text{A4})$$

The diffusion matrix is a diagonal matrix, which is $\mathcal{D} = \text{diag}[(D_t^1 + D_c^1 + D_a^1 + \lambda_{\text{sph}}^1)/2, (D_t^1 + D_c^1 + D_a^1 + \lambda_{\text{sph}}^1)/2, (D_t^2 + D_c^2 + D_a^2 + \lambda_{\text{sph}}^2)/2, (D_t^2 + D_c^2 + D_a^2 + \lambda_{\text{sph}}^2)/2, \kappa_{\text{eff}}, \kappa_{\text{eff}}]$.

Once the covariance matrix V is obtained, the entanglement can then be quantified by means of logarithmic negativity [61]:

$$E_N = \max[0, -\ln 2\tilde{v}_-], \quad (\text{A5})$$

where $\tilde{v}_- = \min \text{eig}|i\Omega_2 \tilde{V}_m|$ ($\Omega_2 = \bigoplus_{j=1}^2 i\sigma_y$ the so-called symplectic matrix and σ_y is the y Pauli matrix) is the minimum symplectic eigenvalue of the covariance matrix $\tilde{V}_m = \mathcal{P}V_m\mathcal{P}$, with V_m the 4×4 covariance matrix associated with the two mechanical modes, and $\mathcal{P} = \text{diag}(1, 1, 1, -1)$ the matrix that inverts the sign of momentum of the second MR, i.e., $p_2 \rightarrow -p_2$, realizing partial transposition at the level of covariance matrices [62].

-
- [1] A. Bassi, K. Lochan, S. Satin, T. P. Singh, and H. Ulbricht, *Rev. Mod. Phys.* **85**, 471 (2013).
- [2] A. Bassi and G. C. Ghirardi, *Phys. Rep.* **379**, 257 (2003); S. L. Adler and A. Bassi, *Science* **325**, 275 (2009).
- [3] G. C. Ghirardi, A. Rimini, and T. Weber, *Phys. Rev. D* **34**, 470 (1986).
- [4] G. C. Ghirardi, P. Pearle, and A. Rimini, *Phys. Rev. A* **42**, 78 (1990); G. C. Ghirardi, R. Grassi, and F. Benatti, *Found. Phys.* **25**, 5 (1995).
- [5] L. Diósi, *Phys. Lett. A* **120**, 377 (1987); *Phys. Rev. A* **40**, 1165 (1989); R. Penrose, *Gen. Relat. Gravit.* **28**, 581 (1996).
- [6] K. Hornberger, S. Gerlich, P. Haslinger, S. Nimmrichter, and M. Arndt, *Rev. Mod. Phys.* **84**, 157 (2012).
- [7] P. Haslinger, N. Dörre, P. Geyer, J. Rodewald, S. Nimmrichter, and M. Arndt, *Nat. Phys.* **9**, 144 (2013).
- [8] M. Bahrani, M. Paternostro, A. Bassi, and H. Ulbricht, *Phys. Rev. Lett.* **112**, 210404 (2014).
- [9] S. Nimmrichter, K. Hornberger, and K. Hammerer, *Phys. Rev. Lett.* **113**, 020405 (2014).
- [10] P. Sekatski, M. Aspelmeyer, and N. Sangouard, *Phys. Rev. Lett.* **112**, 080502 (2014); M. Ho, A. Lafont, N. Sangouard, and P. Sekatski, *New J. Phys.* **18**, 033025 (2016).
- [11] L. Diósi, *Phys. Rev. Lett.* **114**, 050403 (2015).
- [12] J. Li, S. Zippilli, J. Zhang, and D. Vitali, *Phys. Rev. A* **93**, 050102(R) (2016).
- [13] D. Goldwater, M. Paternostro, and P. F. Barker, *Phys. Rev. A* **94**, 010104(R) (2016).
- [14] M. Aspelmeyer, T. J. Kippenberg, and F. Marquardt, *Rev. Mod. Phys.* **86**, 1391 (2014).
- [15] W. Marshall, C. Simon, R. Penrose, and D. Bouwmeester, *Phys. Rev. Lett.* **91**, 130401 (2003); B. Pepper, R. Ghobadi, E. Jeffrey, C. Simon, and D. Bouwmeester, *ibid.* **109**, 023601 (2012).
- [16] O. Romero-Isart, A. C. Pflanzer, F. Blaser, R. Kaltenbaek, N. Kiesel, M. Aspelmeyer, and J. I. Cirac, *Phys. Rev. Lett.* **107**, 020405 (2011); O. Romero-Isart, *Phys. Rev. A* **84**, 052121 (2011).
- [17] J. Bateman, S. Nimmrichter, K. Hornberger, and H. Ulbricht, *Nat. Commun.* **5**, 4788 (2014).
- [18] C. Wan, M. Scala, G. W. Morley, A. A. Rahman, H. Ulbricht, J. Bateman, P. F. Barker, S. Bose, and M. S. Kim, *Phys. Rev. Lett.* **117**, 143003 (2016).
- [19] M. G. Genoni, O. S. Duarte, and A. Serafini, *New J. Phys.* **18**, 103040 (2016).
- [20] S. McMillen, M. Brunelli, M. Carlesso, A. Bassi, H. Ulbricht, M. G. A. Paris, and M. Paternostro, [arXiv:1606.00070](https://arxiv.org/abs/1606.00070).
- [21] S. Mancini, V. Giovannetti, D. Vitali, and P. Tombesi, *Phys. Rev. Lett.* **88**, 120401 (2002).
- [22] D. Vitali, S. Mancini, and P. Tombesi, *J. Phys. A* **40**, 8055 (2007).
- [23] C. Genes, D. Vitali, and P. Tombesi, *New J. Phys.* **10**, 095009 (2008).
- [24] M. J. Hartmann and M. B. Plenio, *Phys. Rev. Lett.* **101**, 200503 (2008).
- [25] J. Zhang, K. C. Peng, and S. L. Braunstein, *Phys. Rev. A* **68**, 013808 (2003).
- [26] J. Li, S. Gröblacher, and M. Paternostro, *New J. Phys.* **15**, 033023 (2013).
- [27] W. Ge, M. Al-Amri, H. Nha, and M. S. Zubairy, *Phys. Rev. A* **88**, 022338 (2013).
- [28] M. Pinar, A. Dantan, D. Vitali, O. Arcizet, T. Briant, and A. Heidmann, *Europhys. Lett.* **72**, 747 (2005).
- [29] S. Pirandola, D. Vitali, P. Tombesi, and S. Lloyd, *Phys. Rev. Lett.* **97**, 150403 (2006).
- [30] K. Borkje, A. Nunnenkamp, and S. M. Girvin, *Phys. Rev. Lett.* **107**, 123601 (2011).
- [31] M. Abdi, S. Pirandola, P. Tombesi, and D. Vitali, *Phys. Rev. Lett.* **109**, 143601 (2012).
- [32] M. J. Woolley and A. A. Clerk, *Phys. Rev. A* **87**, 063846 (2013).
- [33] M. Abdi, S. Pirandola, P. Tombesi, and D. Vitali, *Phys. Rev. A* **89**, 022331 (2014).
- [34] H. Flayac and V. Savona, *Phys. Rev. Lett.* **113**, 143603 (2014).
- [35] Y.-D. Wang and A. A. Clerk, *Phys. Rev. Lett.* **108**, 153603 (2012).
- [36] H. Tan, G. Li, and P. Meystre, *Phys. Rev. A* **87**, 033829 (2013).
- [37] M. J. Woolley and A. A. Clerk, *Phys. Rev. A* **89**, 063805 (2014).
- [38] M. Abdi and M. J. Hartmann, *New J. Phys.* **17**, 013056 (2015).
- [39] L. F. Buchmann and D. M. Stamper-Kurn, *Phys. Rev. A* **92**, 013851 (2015).
- [40] J. Li, I. Moaddel Haghghi, N. Malossi, S. Zippilli, and D. Vitali, *New J. Phys.* **17**, 103037 (2015).
- [41] J. Li, G. Li, S. Zippilli, D. Vitali, and T. C. Zhang, [arXiv:1610.07261](https://arxiv.org/abs/1610.07261).
- [42] S. Belli, R. Bonsignori, G. D'Auria, L. Fant, M. Martini, S. Peirone, S. Donadi, and A. Bassi, *Phys. Rev. A* **94**, 012108 (2016).
- [43] S. Banerjee, S. Bera, and T. P. Singh, *Phys. Lett. A* **380**, 3778 (2016).

- [44] D. E. Chang, C. A. Regal, S. B. Papp, D. J. Wilson, J. Ye, O. Painter, H. J. Kimble, and P. Zoller, *Proc. Natl. Acad. Sci. USA* **107**, 1005 (2010).
- [45] P. F. Barker and M. N. Shneider, *Phys. Rev. A* **81**, 023826 (2010); J. Millen, P. Z. G. Fonseca, T. Mavrogordatos, T. S. Monteiro, and P. F. Barker, *Phys. Rev. Lett.* **114**, 123602 (2015).
- [46] T. Li, S. Kheifets, and M. G. Raizen, *Nat. Phys.* **7**, 527 (2011).
- [47] J. Gieseler, B. Deutsch, R. Quidant, and L. Novotny, *Phys. Rev. Lett.* **109**, 103603 (2012).
- [48] N. Kiesel, F. Blaser, U. Delic, D. Grass, R. Kaltenbaek, and M. Aspelmeyer, *Proc. Natl. Acad. Sci. USA* **110**, 14180 (2013).
- [49] O. Romero-Isart, A. C. Pflanzer, M. L. Juan, R. Quidant, N. Kiesel, M. Aspelmeyer, and J. I. Cirac, *Phys. Rev. A* **83**, 013803 (2011).
- [50] A. C. Pflanzer, O. Romero-Isart, and J. I. Cirac, *Phys. Rev. A* **86**, 013802 (2012).
- [51] S. L. Adler, *J. Phys. A* **40**, 2935 (2007).
- [52] A. Vinante, M. Bahrami, A. Bassi, O. Usenko, G. Wijts, and T. H. Oosterkamp, *Phys. Rev. Lett.* **116**, 090402 (2016).
- [53] M. Bilardello, S. Donadi, A. Vinante, and A. Bassi, *Physica A* **462**, 764 (2016).
- [54] B. Helou, B. Slagmolen, D. E. McClelland, and Y. Chen, [arXiv:1606.03637](https://arxiv.org/abs/1606.03637).
- [55] M. Carlesso, A. Bassi, P. Falferi, and A. Vinante, *Phys. Rev. D* **94**, 124036 (2016).
- [56] A. Vinante, R. Mezzena, and P. Falferi, [arXiv:1611.09776](https://arxiv.org/abs/1611.09776).
- [57] See footnote 7 in F. Laloë, W. J. Mullin, and P. Pearle, *Phys. Rev. A* **90**, 052119 (2014).
- [58] C. Curceanu, B. C. Hiesmayr, and K. Piscicchia, *J. Adv. Phys.* **4**, 263 (2015).
- [59] O. Romero-Isart, L. Clemente, C. Navau, A. Sanchez, and J. I. Cirac, *Phys. Rev. Lett.* **109**, 147205 (2012).
- [60] D. Vitali, S. Gigan, A. Ferreira, H. R. Böhm, P. Tombesi, A. Guerreiro, V. Vedral, A. Zeilinger, and M. Aspelmeyer, *Phys. Rev. Lett.* **98**, 030405 (2007).
- [61] J. Eisert, Ph.D. thesis, University of Potsdam, 2001; G. Vidal and R. F. Werner, *Phys. Rev. A* **65**, 032314 (2002); M. B. Plenio, *Phys. Rev. Lett.* **95**, 090503 (2005).
- [62] R. Simon, *Phys. Rev. Lett.* **84**, 2726 (2000).